https://doi.org/10.20965/jaciii.2015.p0127

Paper:

Speed-Sensorless Vector Control Based on ANN MRAS for Induction Motor Drives

Kai Xu and Shanchao Liu

College of Information Science and Engineering, University of Chongqing Jiaotong
No. 66, Xuefu Rd., Nan'an District, Chonqing 400074, China
E-mail: {xkxjxwx, lscxihuan}@hotmail.com

[Received October 24, 2013; accepted October 27, 2014]

In the speed-sensorless induction motor drives system, Model Reference Adaptive System (MRAS) is the most common strategy. However, speed estimation using reactive power based MRAS has the problem of instability in the regenerating mode of operation. Such estimation technique is simple and has several notable advantages, but is not suitable for induction motor drives. To overcome these problems, a suitable Artificial Neural Networks (ANN) is presented to replace the adjustable model to make the system stable when working at low speed and zero crossing. Simultaneously, in order to enhance the ANN convergence speed and avoid the trap of local minimum value of algorithm, we used the modified Particle Swarm Optimization (PSO) to optimize the weights and threshold values of neural networks. Then the ANN-based MRAS was used to identify the speed of motor in the indirect vector control system. The results of the simulation show that, by this method, the speed of motor can be identified accurately in different situations, and the result is reliable.

Keywords: vector control, speed-sensorless, model reference adaptive system (MRAS), artificial neural networks(ANN), modified particle swarm optimization (PSO)

1. Introduction

Sensorless vector controlled induction motor drives are being vigorously developed for high performance industrial drive systems. Since the elimination of the speed sensor reduces the costs and increases the overall system reliability. On the other hand, the stability at the low speed operation range and the parameter sensitivity can be the main drawbacks of sensorless control [1].

Model Reference Adaptive System (MRAS) is the most common strategy employed due to its relative simplicity. The MRAS is broadly classified as : 1) Rotor Flux (RF), 2) Back-EMF, 3) reactive power, methods. Rotor Flux scheme suffers from stator resistance sensitivity and pure integration problems which may cause DC drift and initial condition problems [2]. Y.Yusof et al. [3] proposed Low-Pass Filters (LPF) with very low cut-off frequency to replace the pure integrator, but it introduces phase and gain errors due to its natural delay. B. Karanayil et al. [4] used a three stage programmable cascaded LPF for the accurate estimation of the rotor flux, whereas it reduces the scheme simplicity. Nonlinear feedback integrators for drift and DC offset compensation have been proposed in [5]. To avoid the problems associated with rotor flux schemes, Back EMF and reactive power schemes have been proposed. Although Back-EMF based techniques avoid pure integration, it may have stability problems at low stator frequency and show low noise immunity [6]. A specially constructed reactive power (Q-MRAS) is presented in [7]. It formulated with instantaneous reactive power in the reference model and steady-state reactive power in the adjustable model. So, it does not require any derivative operations and the flux computation. Moreover, the Q-MRAS is inherently independent of stator resistance variation. However, the Q-MRAS has instability problem in the regenerating mode of operation, as reported in [8]. M. Hinkkanen et al. [9] modifies the error signal to improve the stability in the regenerating mode. A fictitious quantity defined by the outer product of voltage and currents is used in [10] to overcome instability problem under regeneration.

Currently, the Artificial Neural Networks (ANN) [11–14] may be used to improve the performance of the sensorless drives. Shady M.Gadoue et al. [15] proposed a stator current MRAS scheme for speed identification for induction motor drives. This method is complicated because of the application of two neural networks observers. One is current observer and the other is flux observer. The ANN based RF-MRAS is also found in [16]. In [16], the reference model is replaced by an ANN. Generally, the Grads Descend Method (GDM) learning algorithms is used to adjust the neural network weights and threshold values [17]. An algorithm based on Least Mean Square (LMS) method for the training of linear neuron is found in [18]. All the methods mentioned above have the defects of plunging into the local minimum easily, low convergence of rate and bad generalization.

Recently, Zhang Wenli et al. [19] used the Genetic Algorithm (GA) to train the ANN. Particle Swarm Optimization (PSO) is an optimization algorithms based on collective intelligent theory, famous for its strong points

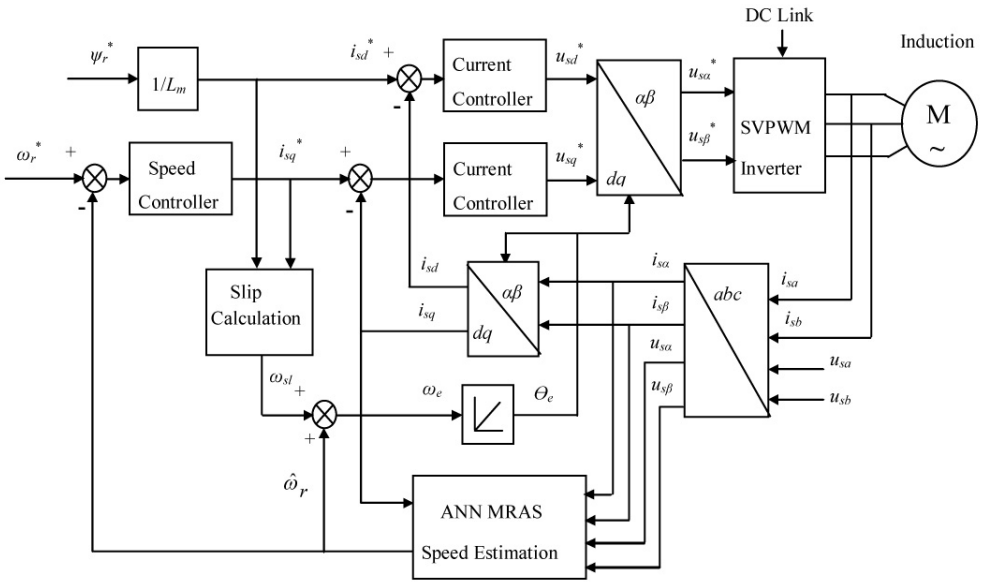

Fig. 1. The schematic diagram of sensorless indirect vector control system.

as follows: quick convergence rate, strong global search ability, omitting the process of gradient computing, and shortening the training time of networks without evolution operation such as: selection, variation etc.

In this paper, firstly, we use a well trained ANN to replace the adjustable model to improve the Q-MRAS scheme performance. The ANN generates accurate reactive power and improved the stability when working at low speed and zero crossing. The proposed method has good speed identification under the regenerating mode. Secondly, we use the modified PSO to optimize the weights and threshold values of ANN. This method can increases the convergence rate and enhance the precision. And finally, the effectiveness of this method is proved by the simulation experiments.

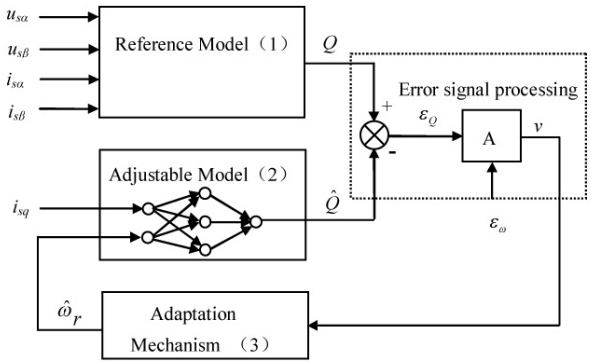

Fig. 2. Q-MRAS speed observer.

2. The Principle of Q-MRAS Speed Observer

The block diagram of a model based sensorless indirect vector control scheme is shown in **Fig. 1**. Based on terminal voltages and currents, the rotor speed is estimated through the proposed ANNbased MRAS. The estimated rotor speed is used for coordinate transformation and to close the speed loop.

The basic concept of MRAS is the presence of a reference model which determines the desired states and an adjustable model which generates the estimated values of the states. The error between these states is fed to an adaptation mechanism to generate an estimated value of the rotor speed which is used to adjust the adaptive model. This process continues till the error between two outputs tends to zero. The structure of the Q-MRAS is shown in **Fig. 2**.

The building blocks of such Q-MRAS are as follows.

Reference model: The reference model computes instantaneous reactive power in stationary reference frame using Eq. (1).

$$Q = u_{s\beta} i_{s\alpha} - u_{s\alpha} i_{s\beta}. \quad \ldots\ldots\ldots\ldots \quad (1)$$

The computation of reactive power in stationary frame does not involve any coordinate transformation. So, the reference model is free from machine parameters.

Adjustable model: Different expressions of reactive power for adjustable model are derived. S. Maiti et al. [2] proposed a detail expressions can be written as :

$$\hat{Q} = \sigma L_s \omega_e \left(i_{sd}^2 + i_{sq}^2\right) + \omega_e \frac{L_m^2}{L_r} i_{sd}^2. \quad \ldots\ldots \quad (2)$$

Where: actual speed of rotor flux $\omega_e = \hat{\omega}_r + \omega_{sl}$, $\hat{\omega}_r$ is the estimated rotor speed, and slip speed $\omega_{sl} = (R_r i_{sq})/(L_r i_{sd})$; σ is the leakage coefficient; i_{sd} and i_{sq} are the d and q components of the stator current vector; R_r is the rotor resistance; L_s, L_m and L_r are the stator, mutual and rotor inductances respectively.

Such Q-MRAS is influenced by the variation of ma-

chine parameters (e.g., rotor resistance) and has unstable when working at low or zero speed operation range. Therefore an artificial neural network is proposed to replace the adjustable model Eq. (2) to improve the Q-MRAS scheme performance at low or zero speed.

Error signal processing: In **Fig. 2**, the reactive power error ε_Q is processed through A, which functions according to the sign of speed error ε_ω and reactive power error ε_Q. The speed error is calculated according to $\varepsilon_\omega = \omega_r^* - \hat{\omega}_r$. The working principle of A is as follows:

$$\text{If } \text{sign}(\varepsilon_\text{Q}) = \text{sign}(\varepsilon_\omega), \text{ then } \text{v} = \varepsilon_\text{Q}, \quad \ldots \quad (3)$$

$$\text{If } \text{sign}(\varepsilon_\text{Q}) \neq \text{sign}(\varepsilon_\omega), \text{ then } \text{v} = -\varepsilon_\text{Q}, \quad \ldots \quad (4)$$

where ε_Q, ε_ω are the inputs and v is the output of the block A. The block is designed to satisfy the Popov's hyper-stability criteria, which tells that the feedforward path gain should be strictly real positive for all speed.

Adaptation mechanism: The reference model Eq. (1) is independent of the motor speed, while the adjustable mode Eq. (2) is speed-dependant. To obtain a stable nonlinear feedback system, a speed tuning signal v and a PI controller are used in the adaptation mechanism to generate the estimated speed. The estimated speed expressions can be written as :

$$\hat{\omega}_r = \left(k_p + \frac{k_i}{s}\right) v, \quad \ldots \quad (5)$$

where k_p and k_i are the proportional coefficient and integral coefficient respectively.

3. ANN for the Computation of $\hat{Q}$

3.1. The ANN Structure Design and Signal Computations

As expressed in Eq. (2), it is observed that $\hat{Q}$ is a function of i_{sd}, i_{sq}, $\hat{\omega}_r$ and ω_{sl}.

$$\hat{Q} = f_1(i_{sd}, i_{sq}, \hat{\omega}_r, \omega_{sl}). \quad \ldots \quad (6)$$

The need of i_{sd} and ω_{sl} may be avoided in the computation of $\hat{Q}$, so the following Eq. (7) is used instead of Eq. (6).

$$\hat{Q} = f_2(i_{sq}, \hat{\omega}_r). \quad \ldots \quad (7)$$

The nonlinear function $f_2(\cdot)$ is unknown to the users. However, the inputs and the corresponding outputs are known. So, the problem relies on the realization of the nonlinear function $f_2(\cdot)$ through input-output mapping. ANN is a well-known tool, which may be used for such purpose.

To obtain good estimation accuracy, the inputs to the network are the present and past values of the q-axis stator current and the estimated rotor speed. To estimate the reactive power in the adjustable model, a 4-13-1 multilayer feedforward neural network is proposed as shown in **Fig. 3**. Variable values like present $i_{sq}(k)$, $\hat{\omega}_r(k)$ and one time step in the past $i_{sq}(k\text{-}1)$, $\hat{\omega}_r(k\text{-}1)$ are treated as the inputs of the ANN. The d-axis stator current i_{sd} and ω_{sl} are not considered as inputs. Generally speaking, The initial

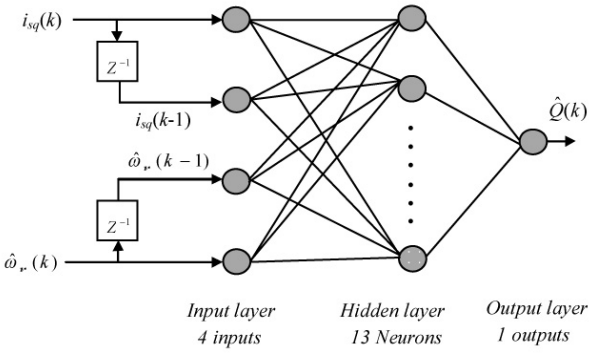

Fig. 3. Structure of the ANN used in the adjustable model.

value of q (the number of nodes of hidden layer) can be obtained according to the empirical formula: $q \geq 2p+1$ (p is the number of nodes of input layer). Finally we make q as 13 through the experiment. The outputlayer consists of only one neuron representing the reactive power for adjustable model.

The various signals at different stages of the network are computed as follows.

Consider a neuron j in a layer m with n inputs in the $(m-1)$ layer, the net input to the neuron is given by:

$$\begin{aligned} net_j &= \sum_{k=1}^{n} w_{jk} x_k + b_j \\ &= w_{j1}x_1 + w_{j2}x_2 + \cdots + w_{jn}x_n + b_j. \end{aligned} \quad \ldots \quad (8)$$

Where w_{jk} is the weight from n inputs in the $(m-1)$ layer to the neuron j, x_k is the k-th output signal in the $(m-1)$ layer to the neuron j, b_j is threshold of the neuron j.

The neuron output is given by:

$$y_j = g(net_j) = g\left(\sum_{k=1}^{n} w_{jk} x_k + b_j\right), \quad \ldots \quad (9)$$

where $g(\cdot)$ is the activation function or the neuron transfer function. The commonest activation functions are: sigmoidal, linear, logsigmoid and tansigmoid activation. Here, we used sigmoidal function in the hidden layer neuron, the neuron transfer function can be written as:

$$y_j = \frac{1}{1+\exp(-net_j)}, \quad \ldots \quad (10)$$

whereas, linear function is considered for the output layer neuron.

3.2. Modified PSO Algorithms

In this paper, a modified PSO training method is proposed. The modified PSO algorithms increases the convergence rate, enhance the precision and avoid the local minimum. The particle in the swarm trails 2 extremum (one optimal solution is found by the particle itself and the other is found by the swarm) in the process of every iteration search to adjust its own position and velocity, finally finishing the optimization. The basic PSO algorithms are

as follows:

$$v_{id}^{k+1} = wv_{id}^{k} + c_1 \times rand_1^k \left(pbest_{id}^k - x_{id}^k \right) + c_2 \times rand_2^k \left(gbest_d^k - x_{id}^k \right) \quad . \quad . \quad . \quad . \quad (11)$$

$$x_{id}^{k+1} = x_{id}^k + v_{id}^{k+1} \quad . \quad . \quad . \quad . \quad . \quad . \quad . \quad . \quad . \quad . \quad . \quad . \quad (12)$$

w: inertia weight, usually $0.4 \sim 1.2$;

v_{id}^k: the d dimensional velocity of the particle i for the k time;

c_1, c_2: acceleration factor, which adjust the longest step width toward the best global particle and the best individual particle. Proper c_1, c_2 can accelerate the convergence rate and not get into the local optimum. Usually $c_1 = c_2 = 2$;

$rand_{1,2}^k$: any value among [0,1];

x_{id}^k: the d dimensional position of the particle i for the k time;

$pbest_{id}^k$: the d dimensional position of the individual extreme point of the particle i for the k time;

$gbest_d^k$: the d dimensional position of global extreme point of the whole swarm for the k time;

v_d: value range is $-v_{d\max}$ to $+v_{d\max}$ in order to prevent the particle from staying away from the search space. If $v_{d\max}$ is too large, the particle will fly away the best solution; If too small, the particle will get into the local optimum. If the d dimension of search space is defined as $[-x_{d\max}, +x_{d\max}]$, then $v_{d\max} = kx_{d\max}$, $0.1 \le k \le 1$.

For practical optimization problems, we often consider the global search first, and make the search space fast enough to converge to an area. Then, we make a careful local search to obtain the high accuracy solution. The study finds that a larger w can strengthen the global search ability, while a smaller w strengthen the local search ability. In this paper, a linear descending algorithms is adopted. w reduces linearly along with the increasing number of iteration. In this way the global search ability is greatly improved. The formula for w is as follows:

$$w = w_{\max} - \frac{w_{\max} - w_{\min}}{iter_{\max}} \times iter. \quad . \quad . \quad . \quad . \quad . \quad (13)$$

$w_{\max} w_{\min}$: maximal and minimal inertia weight, usually $w_{\max} = 0.8 \sim 1.2$, $w_{\min} = 0.4$;

$iter_{\max}$: the maximum number of the iteration set;

$iter$: the current number of iteration.

3.3. The ANN Based on Modified PSO Algorithms

In the process of optimizing ANN, the position vector x is defined as the connection weights and threshold values of the whole ANN. Initialize x and search for the optimal position in the modified PSO method to get theminimal error of mean square:

$$J = E = \frac{1}{N} \sum_i^N \sum_j (d_{ij} - y_{ij})^2. \quad . \quad . \quad . \quad . \quad . \quad . \quad (14)$$

d_{ij}: the expected output value of the particle i through the output layer node j;

y_{ij}: the real output value of the particle i through the output layer node j;

N: the number of sample in the training set.

So, the fitness function is defined as:

$$f = \frac{1}{J}. \quad . \quad . \quad . \quad . \quad . \quad . \quad . \quad . \quad . \quad . \quad . \quad . \quad . \quad . \quad (15)$$

The searching procedures of the proposed modified PSO were shown as below:

Step 1. Initialize the structure of ANN, and set the number of neuron of input, hidden and output layer.

Step 2. Generate initial condition of each agent. Initialize inertia weight w, acceleration factor c_1, c_2, max iteration $N_{\max}$. Velocity of each agent are usually generated randomly within the allowable range. The current searching point is set to pbest for each agent. The best-evaluated value of pbest is set to gbest and the agent number with the best value is stored.

Step 3. The fitness value is calculated for each agent. If the value is better than the current pbest of the agent, the pbest value is replaced by the current value. If the best value of pbest is better than the current gbest, gbest is replaced by the best value and the agent number with the best value is stored.

Step 4. Update the position and velocity of each particle. The current searching point of each agent is changed using Eqs. (11) and (12).

Step 5. Checking the exit condition. If reach to the maximum iteration number $N_{\max}$ or the expected precision, then exit. Otherwise, continue iteration. Go to *Step 3*.

Step 6. The individual that generates the latest is the optimal parameters of the connection weights and threshold values.

To generate the input and output training datas, the vector controlled induction motor running at different speed commands and subjected to various load torques is simulated. 4800 groups of data were obtained and are used to train the ANN. The training is performed off-line using four different algorithms. When the rotate speed ω_r^* is set as 50 r/min, the largest training times is 2000, and the smallest allowable error is 0.005. Comparing modified

Table 1. Error comparing in different algorithms.

Algorithm	Training Times	System Error
GDM-ANN	2000	0.1229
GA-ANN	2000	0.0071
PSO-ANN	2000	0.0065
Modified PSO-ANN	2000	0.0043

Table 2. Weights and bias values.

$W_I\{1,1\}$	0.8539	0.1292	−0.2856	0.7625;	
	0.6291	0.9815	−0.0154	0.6772;	
	0.6630	−0.0410	0.5890	−0.9853;	
	−0.4256	0.1751	0.6573	0.8426;	
	0.5587	−0.1293	0.1372	−0.6971;	
	0.9365	0.0977	−0.1663	−0.9136;	
	−0.2059	0.1182	0.8119	0.8220;	
	0.0360	−0.3363	0.8573	−0.3187;	
	0.2238	0.3745	0.3548	−0.9741;	
	−0.2708	0.2653	0.6189	0.9858;	
	−0.6604	0.6228	−0.0913	0.5713;	
	−0.7660	0.9770	−0.8056	0.9374;	
	0.8147	0.1565	−0.6526	0.1671;	
$W_L\{2,1\}$	0.7091	0.3674	−0.5289	0.7849	−0.5464
	−0.0163	0.9845	−0.4055	−0.7826	0.6576
	0.3896	−0.8098	0.1437		
$b\{1\}$	0.9080	−0.2026	0.5942	0.2109	−0.9495
	−0.2869	−0.1726	0.0527	−0.6473	0.4079
	0.2270	−0.0168	0.0202		
$b\{2\}$	−0.3607				

PSO-ANN with the Gradient Descent with Momentum to optimize ANN (GDM-ANN), Genetic Algorithm to optimize ANN (GAANN) and the basic PSO-ANN, it's easy to obtain the conclusion that modified PSO-ANN is the best of all. It has a smaller net error and quick convergent rate under the same iterating times. The comparing result is shown in **Table 1**.

The ANN is trained using modified PSO, the optimized parameters of ANN are shown in **Table 2**.

Where $W_I\{1,1\}$ are the weights to the hidden layer 1 from input 1, $W_L\{2,1\}$ are the weights to the output layer 2, $b\{1\}$ and $b\{2\}$ are the bias to the hidden layer 1 and output layer 2 respectively.

The well-trained ANN is used in the adjustable model of the Q-MRAS to deliver accurate reactive power under all operating conditions. This will benefit from the following advantages: fault tolerance, noise immunity and fast processing speed.

4. System Simulation Results

In this section, the software Matlab is used to simulate the whole system to examine the performance of the ANN-based Q-MRAS. Through a lot of experiments, the parameters of modified PSO used in the simulation experiments are as followings: $\omega_{\max} = 0.9$, $\omega_{\min} = 0.4$, $c_1 = 2$, $c_1 = 1.8$, the number of the particles is 40, the dimension of particles is 79. For a induction motor, with the following parameters: $P_n = 2.2$ kW, $U_n = 380$ V, $p = 2$, $f_n = 50$ Hz, $R_s = 0.435\ \Omega$, $R_r = 0.816\ \Omega$, $L_s = L_r = 2.08$ mH, $L_m = 69.4$ mH, $J = 0.18$ kg·m^2.

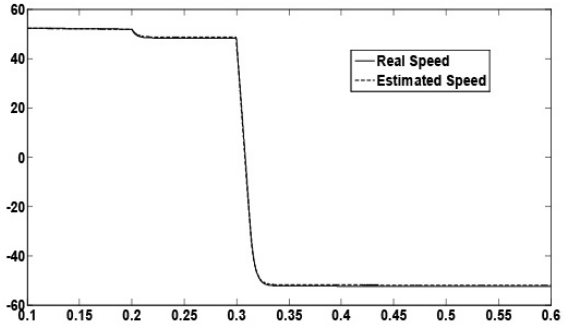

Fig. 4. Real and estimated speed at low speed.

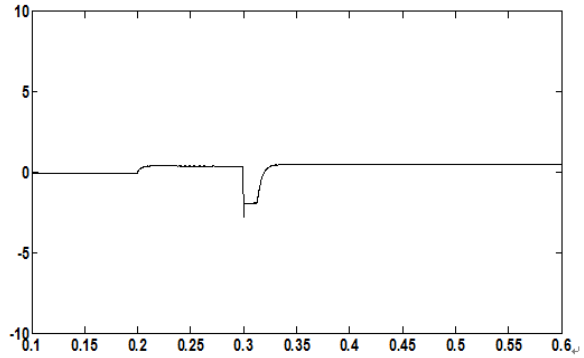

Fig. 5. Speed error curve at low speed.

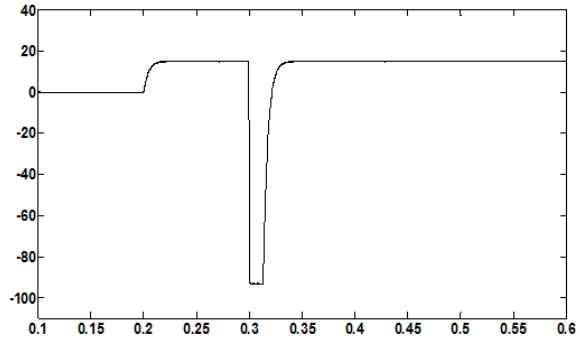

Fig. 6. Electromagnetic torque at low speed.

In the simulation, the error of the speed estimation through the ANN is checked. The following several cases include low and high speed, slow zero crossing, and operation in the regenerating mode. Simultaneously, the disturbance of the load is considered. The estimated speed and real speed curves of the method are given, and the electromagnetic torque curves are also presented.

4.1. Low Speed and Zero Crossing Operation

Figures 4–6 show the simulation results of command speed ω_r^* change from 50 r/min to −50 r/min at 0.3 s. The load disturbance set at 15 N·m suddenly at 0.2 s.

Figure 4 is the comparison between the real speed and estimated speed. **Fig. 5** is the speed error curve. It is observed that the estimated speed follows the real speed with good accuracy. Even in the instant load, it reflects negligible speed estimation error. In the dynamic process, the slow zero crossing has taken place at 0.31 s, and the estimated speed error does not exceed −2.5 r/min. The results reveal satisfactory performance around zero crossing. The performance of the Q-MRAS around zero crossing is improved when the djustable model is replaced by the well trained ANN. The well trained ANN generates accurate reactive power at regeneration. As a result, the proposed method also has good speed identification at low speed and zero crossing.

Figure 6 is the electromagnetic torque curve. The electromagnetic torque is matched with the load torque. The estimated speed and torque follow the command speed and torque with sufficient accuracy, which reveals that the drive enters into the generating mode stability.

4.2. Dynamic and Static Characteristics

Figures 7–9 show the simulation results of speed change from static to 1100 r/min. The load disturbance set at 85 N·m suddenly at 0.4 s, and unloading at 0.6 s.

Figure 7 is the comparison between real speed and estimated speed in high speed. It is noticed that both of them are closely following. **Fig. 8** is the speed error curve. By analyzing the waveforms, although there are errors always in the dynamic process, the estimated speed error does not exceed -3.4%, and the estimated speed can rapidly track the real speed. When reached a speed of 1100 r/min, the estimated speed is very precise in steady state. Small deviation between the real speed and estimated speed is noticed only in the instant heavy load at 0.4 s. When removing the load at 0.6 s, the estimated speed is in good accordance with the real speed. So the proposed method has high accurate and strong robustness in high speed.

Figure 9 is the electromagnetic torque curve. From 0.4 to 0.8 s, the torque keeps balance. Although there are tiny amplitude vibrates in the steady state, the electromagnetic torque is matched with the load torque.

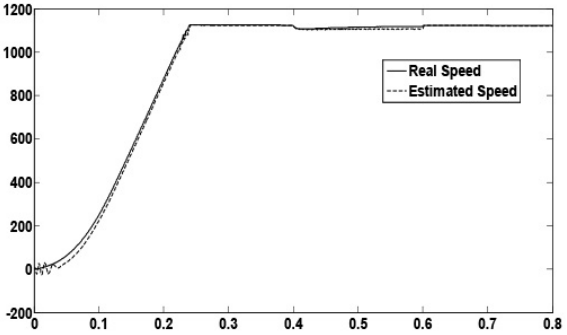

Fig. 7. Real and estimated speed at high speed.

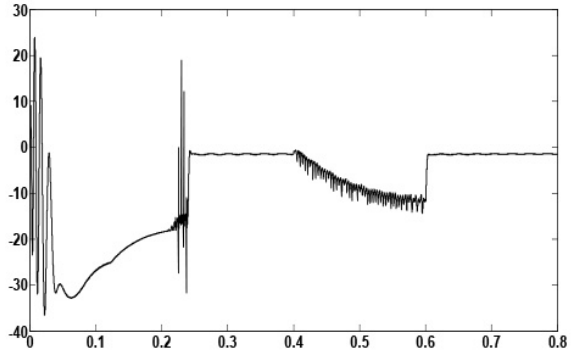

Fig. 8. Speed error curve at high speed.

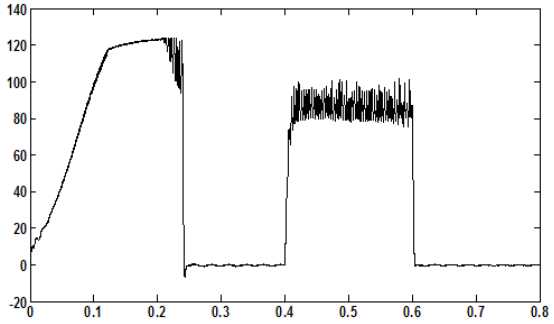

Fig. 9. Electromagnetic torque at high speed.

5. Conclusions

Speed estimation using reactive power based MRAS has the problem of instability in the regenerating mode of operation. In this paper, a suitable ANN to replace the adjustable model to make the system stable when working at low speed and zero crossing. Furthermore, in order to enhance the ANN convergence speed and avoid the trap of local minimum value of algorithms, we used a modified PSO to optimize the weights and threshold values of neural networks. Results show that, the well trained ANN estimates rotor speed accurately at regeneration. In the dynamic and static respond process, the new strategy has accurate speed estimation, as well as enhances the robustness in the sensorless indirect vector control system.

Further research should focus on some new evolutionary computing approaches to optimize the ANN parameters, such as artificial fish swarm algorithm, ant colony optimization, and so on. Simultaneously, the evolutionary computation should be combined with other intelligent control method to solve some practical problems.

References:

[1] J. Holtz and J. Quan, "Drift and parameter compensated flux estimator for persistent zero stator frequency operation of sensorless controlled induction motors," IEEE Trans. Industry Applications, Vol.39, No.4, pp. 1052-1060, 2003.

[2] P. Vas, "Sensorless vector and direct torque control," Oxford University Press, 1998.

[3] Y. Yusof and A. H. M. Yatim, "Simulation and modelling of stator flux estimator for induction motor using artificial neural network technique," Proc. of National Power and Energy Conf. pp. 11-15, 2003.

[4] B. Karanayil, M. F. Rahman, and C. Grantham, "An implementation

of a programmable cascaded low-pass filter for a rotor flux synthesizer for an induction motor drive," IEEE Trans. on Power Electron., Vol.19, No.2, pp. 257-263, 2004.

[5] Q. Gao, C. S. Staines, G. M. Asher, and M.Sumner, "Sensorless speed operation of cage induction motor using zero drift feedback integration with MRAS observer," Proc. European Conf. on Power Electronics and Applications, 2005.

[6] M. Rashed and A. F. Stronach, "A stable back-EMF MRAS-based sensorless low speed induction motor drive insensitive to stator resistance variation," IEEE Proc. Electr. Power Appl., Vol.l51, No.6, pp. 685-693, 2004.

[7] S. Maiti, C. Chakraborty, Y. Hori, and M. C. Ta, "Model reference adaptive controller-based rotor resistance and speed estimation techniques for vector controlled induction motor drive utilizing reactive power," IEEE Trans. Ind. Electron., Vol. 55, No.2, pp. 594-601, 2008.

[8] S. Maiti and C. Chakraborty, "Experimental validation of very-low and zero speed operation of a flux-eliminated adaptive estimator for vector controlled IM drive," Proc. Conf. Rec. IEEE ICIT, pp. 1-6, 2009.

[9] M. Hinkkanen, L. Harnefors, and J. Luomi, "Reduced-order flux observers with stator-resistance adaptation for speed-sensorless induction motor drives," IEEE Trans. Power Electron., Vol.25, No.5, pp.1173-1183, 2010.

[10] A. V. R. Teja, C. Chakraborty, S. Maiti, and Y.Hori, "A new model reference adaptive controller for four quadrant vector controlled induction motor drives," IEEE Trans. Ind. Electron., Vol.59, No.10, pp. 3757-3767, 2012.

[11] Y. Sayouti, A. Abbou, M. Akherraz, and H. Mahmoudi, "Sensorless low speed control with ANN MRAS for direct torque controlled induction motor drive," Proc. of the 2011 Int. Conf. on Power Engineering, Energy and Electrical Drives, pp. 623-628, 2011.

[12] A. Accetta, M. Cirrincione, M. Pucci, and G. Vitale, "Sensorless control of PMSM fractional horsepower drives by signal injection and neural adaptive-band filtering," IEEE Trans. on Industrial Electronics, Vol.59, pp. 1355-1366, 2012.

[13] W. Gao and Z. Guo, "Speed sensorless control of PMSM using model reference adaptive system and RBFN," J. of networks, Vol.8, No.1, pp. 213-219, 2013.

[14] T. Orlowska-Kowalska and M. Kaminski, "FPGA implementation of the multilayer neural network for the speed estimation of the two-mass drive system," IEEE Trans. Ind. Informat., Vol.7, No.3, pp. 436-445, 2011.

[15] S. M. Gadoue, D. Giaouris, and J. W. Finch, "A neural network based stator current MRAS observer for speed sensorless induction motor drives," Proc. Industrial Electronics, pp. 650-655, 2008.

[16] K. Xu and X. Pingwang, "Speed sensorless vector control with wavelet neural network for induction motor drive," Proc. ICIC Express Letters, Vol.8, No.9, pp. 2431-2436, 2014.

[17] Y. Xiaoting and Z. Qingchun, "Speed estimation of induction motor based on neural network," Proc. of the 2nd Int. Conf. on Intelligent Control and Information Processing, pp. 619-623, 2011.

[18] C. Wenhao and C. Jiangxia, "Speed identification method in direct torque control of asynchronous machine based on neuron network theory," Proc. of the 2012 Int. Conf. on Computer Application and System Modeling, pp. 133-136, 2012.

[19] Z. Wenli and L. Guorong, "Research of speed observer based on BP neural network optimized by Genetic Algorithm," Proc. Computer Engineering and Applications, Vol.49, No.12, pp. 259-266, 2013.

[20] S. Maiti and Y. Hori, "An dadptive speed sensorless induction motor drive with artificial neural network for stability enhancement," IEEE Trans. on Industrial Informatics, Vol.8, No.4, pp.757-766, 2012.

Name:
Kai Xu

Affiliation:
Professor, Collegeof Information Science and Engineering, University of Chongqing Jiaotong

Address:
No. 66, Xuefu Rd., Nan'an District, Chongqing 400074, China

Brief Biographical History:
1993-2007 Senior engineer in Xichang Satellite Launching Center
2002- M.Sc. in Control Science and Engineering, Chongqing University
2008- Professor in the Chongqing Jiaotong University.

Main Works:
• "The Intelligent Integrated Speed Controller of DTC for Induction Motor," Artificial Life and Robotics, Vol.19, No1, pp. 33-39, 2014.

Membership in Academic Societies:
• Expert commissioner of Chongqing Science and Technology Commission
• Expert commissioner of Chongqing Construction Commission

Name:
Shanchao Liu

Affiliation:
College of Electromechanical and Automotive Engineering, University of Chongqing Jiaotong

Address:
No. 66, Xuefu Rd., Nan'an District, Chongqing 400074, China

Brief Biographical History:
2009- Received Bachelor's degree from Electrical Engineering and Automation, Chongqing Jiaotong University
2013- Postgraduate student, Traffic Electrical Equipment and Control, Chongqing Jiaotong University

Main Works:
• An online adaptive PSS based on RBF neural network identifier," J. WSEAS Trans. on Systems and Control, Vol.9, pp. 379-387. 2014.